An Optimality Analysis of Sensor-Target Geometries for Signal Strength Based Localization

Adrian N. Bishop and Patric Jensfelt

Royal Institute of Technology (KTH)
Stockholm, Sweden
adrianb@kth.se, patric@kth.se

***Abstract*—In this paper we characterize the bounds on localization accuracy in signal strength based localization. In particular, we provide a novel and rigorous analysis of the relative receiver-transmitter geometry and the effect of this geometry on the potential localization performance. We show that uniformly spacing sensors around the target is not optimal if the sensor-target ranges are not identical and is not necessary in any case. Indeed, we show that in general the optimal sensor-target geometry for signal strength based localization is not unique.**

I. Introduction

The characteristics of the radio channel between a transmitter and a number of fixed location base stations are dependent on the location of the transmitter [1]. As such, we can exploit certain known characteristics of the channel in order to estimate the transmitter's location [2], [3]. In particular, the received signal strength (RSS) at a number of receivers (or sensors) permits passive localization of an emitter/target (or transmitter) whose transmission power is known[1]. As such, RSS-based localization has been considered as a promising technology for providing location information in sensor networks [4], mobile/wireless computing [5] and cellular phone networks [6] etc.

Given any localization technology (i.e. bearing, time-of-arrival, RSS etc [3]), it is well known that the relative sensor-target geometry can significantly affect the potential performance of any particular localization algorithm [7]–[11]. Noting that the Cramer-Rao lower bound is a function of the relative sensor-target geometry [12], a number of authors have attempted to identify those geometric sensor configurations which minimize some measure of this variance lower bound; see [7]–[9], [13]. The idea is that such geometric configurations are likely to result in accurate localization (at least for efficient estimation algorithms). In [7]–[9], the optimal localization geometry is characterized for range-only, bearing-only and time-of-arrival localization respectively.

In this paper, the fundamental limits on the accuracy of received signal strength (RSS) based localization [1], [4] are examined. The Fisher information matrix (and consequently the Cramer-Rao bound) is derived in terms of the relative receiver-transmitter angular geometry. Then a rigorous (and novel) characterization of the geometry is given with arbitrary receiver-transmitter ranges and arbitrary path loss exponents and shadowing statistics for each receiver channel. In this paper we prove that placing sensors with a uniform angular separation around the target is suboptimal in general. Moreover, we provide a practically important result stating that the optimal sensor configuration is generally not unique and can always be constructed with all sensors on a single half-plane with respect to the target.

The Cramer-Rao bound for RSS-based localization is also derived in [4], [14]–[17] (albeit not in terms of the angular receiver-transmitter relationships). However, in [4], [14]–[17] the connection between the variance lower-bound and the transmitter-receiver geometry is not explicitly examined and no attempt is made to optimize this relationship. Indeed, no existing work in the literature explicitly considers the problem of optimal sensor placement for RSS-based localization.

This paper is organized as follows. In the next section, the notation and RSS-based localization problem is introduced along with the Cramer-Rao inequality and the Fisher information matrix for RSS-based localization. In Section III the localization geometry is briefly examined with two sensors. Then in Section IV the localization geometry for RSS-based localization is analyzed for an arbitrary number of sensors with a number of important results presented. In Section V we return to the important case of three sensors and completely characterize the localization geometry given arbitrary system parameters and sensor-target ranges. We then examine an illustrative example with three sensors. In Section VI and VII we provide a short discussion and conclusion.

II. The Cramer-Rao Inequality, Fisher Information and Received Signal Strength

Consider a target emitter with an unknown position $\mathbf{x} = [x_1\ x_2]^{\mathrm{T}} \in \mathbb{R}^2$. Consider n receivers (called sensors) in known positions given by $\mathbf{s}_i = [s_{i1}\ s_{i2}]^{\mathrm{T}} \in \mathbb{R}^2$, $\forall i \in \{1, \ldots, n\}$. Let $\phi_i(\mathbf{x}) \in [0, 2\pi)$ denote the bearing of the emitter taken counter-clockwise from the positive s_{i1}-direction. The angle subtended at the emitter by two sensors i and j is denoted by $\vartheta_{ij} = \vartheta_{ji} \in [0, \pi]$. The geometry of RSS-based localization is illustrated in Fig. 1 with $n = 2$ sensors[2].

The RSS (in dBm) measured at the i^{th} sensor obeys

$$\widehat{p}_i = p_i + v_i = p_0 - 10\alpha_i \log_{10}\left(\|\mathbf{x} - \mathbf{s}_i\|\right) + v_i \qquad (1)$$

[1]It is even possible to relax the assumption of a known transmission power, albeit we do not discuss this point further in this paper.

[2]Note that although we consider 2D scenarios for theoretical reasons, the results provided in this paper can be interpreted heuristically in 3D as good *rules-of-thumb* when the the sensor-target range (in an arbitrary plane) is large.

Cite as: A.N. Bishop and P Jensfelt, "Optimality Analysis of Sensor-Target Geometries for Signal Strength Based Localization", in Proceedings of the 5th International Conference on Intelligent Sensors, Sensor Networks, and Information Processing (ISSNIP'07), pages 127-132, Melbourne, Australia, December, 2009.

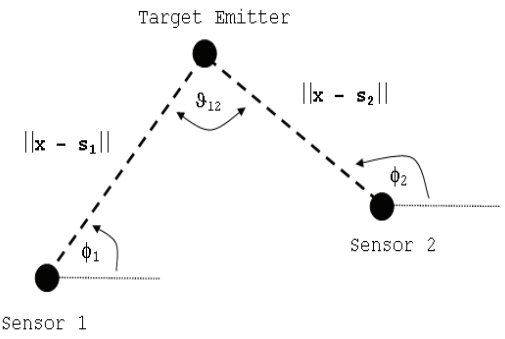

Fig. 1. A typical RSS-based localization scenario with two sensors.

where $\widehat{p}_i$ is the measured RSS and p_0 is the RSS calculated at a 1 unit reference distance using the free-space Friis model. Here, the assumed known α_i is the relevant path loss exponent. Finally, v_i is a Gaussian random variable with known variance σ_i^2 used to model shadowing and fading effects. For generality we allow $\alpha_i \neq \alpha_j$ and $\sigma_i^2 \neq \sigma_j^2$ when $i \neq j$. For n sensors we get,

$$\widehat{\mathbf{p}} = \mathbf{p} + \mathbf{v} = [p_1 \ \ldots \ p_n]^{\mathrm{T}} + [v_1 \ \ldots \ v_n]^{\mathrm{T}} \tag{2}$$

which obeys $\widehat{\mathbf{p}} \sim \mathcal{N}(\mathbf{p}, \mathbf{R_p})$ with covariance matrix $\mathbf{R_p} = \mathrm{diag}\left(\sigma_1^2, \ldots, \sigma_n^2\right)$. If $\mathcal{I}(\mathbf{x})$ is the Fisher information matrix then the Cramer-Rao bound for an *unbiased* estimate $\widehat{\mathbf{x}}$ of $\mathbf{x}$ states that $\mathrm{E}\left[(\widehat{\mathbf{x}} - \mathbf{x})(\widehat{\mathbf{x}} - \mathbf{x})^{\top}\right] \geq \mathcal{I}(\mathbf{x})^{-1}$. If $\mathcal{I}(\mathbf{x})$ is singular then (in general) no unbiased estimator for $\mathbf{x}$ exists with a finite variance [12]. The $(i,j)^{th}$ element of $\mathcal{I}(\mathbf{x})$ is given by

$$\left(\mathcal{I}\left(\mathbf{x}\right)\right)_{i,j} = E\left[\frac{\partial}{\partial x_i} \ln\left(f_{\widehat{\mathbf{p}}}(\widehat{\mathbf{p}};\mathbf{x})\right) \frac{\partial}{\partial x_j} \ln\left(f_{\widehat{\mathbf{p}}}(\widehat{\mathbf{p}};\mathbf{x})\right)\right] \tag{3}$$

where $\mathbf{x} = [x_1 \ x_2]^{\mathrm{T}}$ and $f_{\widehat{\mathbf{p}}}(\widehat{\mathbf{p}};\mathbf{x})$ is the Gaussian likelihood function. We then easily find $\mathcal{I}(\mathbf{x}) = \nabla_{\mathbf{x}}\mathbf{p}(\mathbf{x})^{\mathrm{T}}\mathbf{R}_{\mathbf{p}}^{-1}\nabla_{\mathbf{x}}\mathbf{p}(\mathbf{x})$. After some algebra, the Fisher information matrix for n sensors can be given by

$$\mathcal{I}\left(\mathbf{x}\right) = \kappa \sum_{i=1}^{n} \begin{bmatrix} \frac{\beta_i \cos^2(\phi_i(\mathbf{x}))}{\|\mathbf{x}-\mathbf{s}_i\|^2} & \frac{\beta_i \sin(2\phi_i(\mathbf{x}))}{2\|\mathbf{x}-\mathbf{s}_i\|^2} \\ \frac{\beta_i \sin(2\phi_i(\mathbf{x}))}{2\|\mathbf{x}-\mathbf{s}_i\|^2} & \frac{\beta_i \sin^2(\phi_i(\mathbf{x}))}{\|\mathbf{x}-\mathbf{s}_i\|^2} \end{bmatrix} \tag{4}$$

where $\beta_i = \frac{\alpha_i^2}{\sigma_i^2}$, $\kappa = \frac{100}{\ln^2(10)}$ and i indexes over the sensors. The particular form of the Fisher information matrix given in this paper (4) is a novel contribution in RSS-based localization. This form is designed to aid in finding the optimal sensor *angular positions*. Note that $\det\left(\mathcal{I}(\mathbf{x})\right)$ is inversely proportional to the uncertainty area of an unbiased estimate of $\mathbf{x}$ [12]. We use $\det\left(\mathcal{I}(\mathbf{x})\right)$ to analyze the sensor-emitter geometry and establish which sensor configurations minimize the variance achievable by an efficient estimator. The mean-squared-error (MSE) of an unbiased estimator is lower bounded by the trace of the Cramer-Rao given by

$$\begin{aligned} \mathrm{MSE} &\geq \frac{\left(\mathcal{I}\left(\mathbf{x}\right)\right)_{1,1} + \left(\mathcal{I}\left(\mathbf{x}\right)\right)_{2,2}}{\det(\mathcal{I}(\mathbf{x}))} \\ &\geq \frac{\kappa}{\det(\mathcal{I}(\mathbf{x}))} \sum_{i=1}^{n} \frac{\beta_i}{\|\mathbf{x}-\mathbf{s}_i\|^2} \end{aligned} \tag{5}$$

In this paper we are not constructing estimators but rather characterizing the effect of the localization geometry on the performance of a generic efficient estimator. In practice, this analysis can serve as a guide for sensor placement with biased estimators, or given estimates $\widehat{\mathbf{x}}$ of the true target location $\mathbf{x}$.

Theorem 1: Let $\|\mathbf{x} - \mathbf{s}_i\|$ and $\beta_i = \frac{\alpha_i^2}{\sigma_i^2}$ be arbitrarily fixed $\forall i$. The following optimization problems are equivalent:

(i) $\mathrm{argmax}_{\phi_1,\ldots,\phi_n} \det\left(\mathcal{I}(\mathbf{x})\right)$;

(ii) $\mathrm{argmin}_{\phi_1,\ldots,\phi_n} \left(\sum_1^n \frac{\beta_i \sin(2\phi_i)}{\|\mathbf{x}-\mathbf{s}_i\|^2}\right)^2 + \left(\sum_1^n \frac{\beta_i \cos(2\phi_i)}{\|\mathbf{x}-\mathbf{s}_i\|^2}\right)^2$;

(iii) $\mathrm{argmin}_{\phi_1,\ldots,\phi_n} \left|\sum_{i=1}^n \frac{\beta_i}{\|\mathbf{x}-\mathbf{s}_i\|^2} e^{2j\phi_i(\mathbf{x})}\right|^2, j = \sqrt{-1}$;

(iv) $\mathrm{argmax}_{\phi_1,\ldots,\phi_n} \sum_{\mathcal{S}} \frac{\beta_i\beta_j \sin^2(\phi_i - \phi_j)}{\|\mathbf{x}-\mathbf{s}_i\|^2\|\mathbf{x}-\mathbf{s}_j\|^2}, \mathcal{S} = \{\{i,j\}\}$;

where $\beta_i = \frac{\alpha_i^2}{\sigma_i^2}$ and $\mathcal{S} = \{\{i,j\}\}$ is the set of all combinations of i and j with $i,j \in \{1,\ldots,n\}$ and $i > j$ and $|\mathcal{S}| = \binom{n}{2}$.

Proof: Note that (iii) follows from (ii) by Euler's formula. Hence, we need to show the equivalence of (ii) and (i), and (iv) and (i). We find that (4) can be rewritten as

$$\mathcal{I}\left(\mathbf{x}\right) = \kappa \begin{bmatrix} \sum_1^n \frac{\beta_i(1+\cos(2\phi_i(\mathbf{x})))}{2\|\mathbf{x}-\mathbf{s}_i\|^2} & \sum_{i=1}^n \frac{\beta_i \sin(2\phi_i(\mathbf{x}))}{2\|\mathbf{x}-\mathbf{s}_i\|^2} \\ \sum_{i=1}^n \frac{\beta_i \sin(2\phi_i(\mathbf{x}))}{2\|\mathbf{x}-\mathbf{s}_i\|^2} & \sum_1^n \frac{\beta_i(1-\cos(2\phi_i(\mathbf{x})))}{2\|\mathbf{x}-\mathbf{s}_i\|^2} \end{bmatrix} \tag{6}$$

where $\beta_i = \frac{\alpha_i^2}{\sigma_i^2}$, $\kappa = \frac{100}{\ln^2(10)}$ and such that

$$\begin{aligned} \det\left(\mathcal{I}\left(\mathbf{x}\right)\right) = \frac{\kappa^2}{4} \Bigg[&\left(\sum_{i=1}^n \frac{\beta_i}{\|\mathbf{x}-\mathbf{s}_i\|^2}\right)^2 - \\ &\left(\sum_{i=1}^n \frac{\beta_i \cos\left(2\phi_i(\mathbf{x})\right)}{\|\mathbf{x}-\mathbf{s}_i\|^2}\right)^2 - \left(\sum_{i=1}^n \frac{\beta_i \sin\left(2\phi_i(\mathbf{x})\right)}{\|\mathbf{x}-\mathbf{s}_i\|^2}\right)^2 \Bigg] \end{aligned} \tag{7}$$

which directly implies the equivalence of (ii) and (i). Now let $\mathbf{R}_{\mathbf{p}}^{-1/2} = \mathrm{diag}\left(\sigma_1^{-1}, \ldots, \sigma_n^{-1}\right)$ and $\mathbf{G} = \mathbf{R}_{\mathbf{p}}^{-1/2}\nabla_{\mathbf{x}}\mathbf{p}(\mathbf{x})$ such that $\mathcal{I}(\mathbf{x}) = \mathbf{G}^{\mathrm{T}}\mathbf{G}$. We then also have

$$\det\left(\mathcal{I}\left(\mathbf{x}\right)\right) = \kappa^2 \det\left(\mathbf{G}^{\mathrm{T}}\mathbf{G}\right) = \kappa^2 \sum_{k=\{1,\ldots,\binom{n}{2}\}} \det\left(\mathbf{G}_k\right)^2 \tag{8}$$

from the Cauchy-Binet formula [18] and $\mathbf{G}_k$ is a 2×2 minor of $\mathbf{G}$ taken from the set of minors indexed by $\mathcal{S} = \{\{i,j\}\}$. All 2×2 minors of $\mathbf{G}$ can be given as

$$\mathbf{G}_{\mathcal{S}} = \begin{bmatrix} \frac{\alpha_i}{\sigma_i\|\mathbf{x}-\mathbf{s}_i\|}\cos(\phi_i(\mathbf{x})) & \frac{\alpha_i}{\sigma_i\|\mathbf{x}-\mathbf{s}_i\|}\sin(\phi_i(\mathbf{x})) \\ \frac{\alpha_j}{\sigma_j\|\mathbf{x}-\mathbf{s}_j\|}\cos(\phi_j(\mathbf{x})) & \frac{\alpha_j}{\sigma_j\|\mathbf{x}-\mathbf{s}_j\|}\sin(\phi_j(\mathbf{x})) \end{bmatrix} \tag{9}$$

where $\mathcal{S} = \{\{i,j\}\}$ with $|\mathcal{S}| = \binom{n}{2}$ can be considered the set of all combinations of i and j with $i > j$. Now the equivalence of (iv) and (i) follows with $\beta_i = \frac{\alpha_i^2}{\sigma_i^2}$. ∎

Any sensor-emitter configuration that solves the problems in Theorem 1 is called an *optimal sensor configuration* and we will phrase such configurations in terms of the angles $\vartheta_{ij} = \vartheta_{ji} \in [0, \pi]$. The optimal configuration is not generally unique given arbitrary sensor-emitter ranges.

Corollary 1: Reflecting a sensor about the emitter position, i.e. moving a sensor from $\mathbf{s}_i$ to $2\mathbf{x} - \mathbf{s}_i$, does not affect the value of the Fisher information determinant.

Proof: Substituting $2\mathbf{x}-\mathbf{s}_i$ for $\mathbf{s}_i$ in (7) does not affect $\|\mathbf{x}-\mathbf{s}_i\|^2$ or the value of $\cos(2\phi_i(\mathbf{x}))$ or $\sin(2\phi_i(\mathbf{x}))$. ■

Importantly, Corollary 1 indicates that an optimal sensor-target configuration can be formed with all sensors located on a single half-plane with respect to the true target location. Naturally, this result simplifies the design problem of optimal sensor placement considerably in many cases, e.g. where 'surrounding' the transmitter with sensors is not feasible.

The optimization problems in Theorem 1 can be solved on-the-fly in practice and they can be used to derive control laws for mobile sensors (which typically use an estimated value $\widehat{\mathbf{x}}$ of $\mathbf{x}$). Given only an estimate $\widehat{\mathbf{x}}$ of $\mathbf{x}$, the subsequent results on optimal sensor configurations can be used to (re-)arrange sensors in a manner which can considerably improve recursive localization performance. The given results can also indicate how much performance gain will be obtained by moving sensors along a specific trajectory (relative to $\mathbf{x}$ or $\widehat{\mathbf{x}}$). A fundamental characterization can be used by an external observer (or user/designer) to ascertain fundamental reasons for poor localization performance in a straightforward and intuitive manner. Subsequently, our focus is on explicitly analyzing the relative geometry in order to analytically characterize the actual optimal geometrical relationships.

III. The Optimal Geometry with Two Sensors

When $n=2$, the determinant (7) does not generally vanish. However, a binary ambiguity generally exists in an estimate of $\mathbf{x}$. The next result completely characterizes the optimal sensor configuration with $n=2$ sensors[3].

Proposition 1: Suppose that $\|\mathbf{x}-\mathbf{s}_i\|$ *and* $\beta_i=\frac{\alpha_i^2}{\sigma_i^2}$ *are arbitrarily fixed* $\forall i\in\{1,2\}$. *The determinant* $\det(\mathcal{I}(\mathbf{x}))$ *is maximized when* $\vartheta_{12}=\vartheta_{21}=\frac{\pi}{2}$ *and the maximum is independent of* $\|\mathbf{x}-\mathbf{s}_i\|$ *and* β_i.

Proof: Let $\gamma_i=\beta_i/\|\mathbf{x}-\mathbf{s}_i\|^2$ and with no loss of generality let $\gamma_2=c\gamma_1$ for some constant $c>0$. Then from Theorem 1 (ii) we want to find the minimum of

$$\gamma_1^2\left[\left(\sin(2\phi_1)+c\sin(2\phi_2)\right)^2+\left(\cos(2\phi_1)+c\cos(2\phi_2)\right)^2\right]$$
$$=\gamma_1^2\left[1+c+c\cos\left(2\phi_1(\mathbf{x})-2\phi_2(\mathbf{x})\right)\right]$$

which occurs when $\cos(2\phi_1-2\phi_2)=-1$. Thus, $\phi_2-\phi_1=k\pi-\frac{\pi}{2}$ for $k\in\mathbb{N}$ and the angle subtended at the emitter by the sensors is $\vartheta_{12}=\vartheta_{21}=(\phi_2-\phi_1)\mathrm{mod}(\pi)=\frac{\pi}{2}$. ■

In the remainder of this paper we assume $n\geq 3$ since the special case of $n=2$ does not follow straightforwardly.

[3]Although the optimal configuration with $n=2$ sensors is intuitively expected, there does not appear to be a general proof in the literature for RSS-based localization. For completeness, we use the framework given in Theorem 1 to derive the optimal angular configuration for localization with $n=2$ sensors. We then move to the case where $n\geq 3$ and analyze the optimal angular configurations for localization. The case $n\geq 3$ does not follow directly, and cannot be easily intuited, from any existing literature on RSS-based localization. As we will show, the idea that uniformly spacing sensors around the target is optimal is generically incorrect and never necessary.

IV. Results on the Optimal RSS Localization Geometry with N Sensors

Firstly, we consider the special case where $\|\mathbf{x}-\mathbf{s}_i\|=\|\mathbf{x}-\mathbf{s}_j\|$ and $\beta_i=\beta_j$ are arbitrary $\forall i,j\in\{1,\ldots,n\geq 3\}$.

Theorem 2: Suppose that $\|\mathbf{x}-\mathbf{s}_i\|=\|\mathbf{x}-\mathbf{s}_j\|=r$ *and* $\beta_i=\beta_j=\beta$ *are fixed (but arbitrary)* $\forall i,j\in\{1,\ldots,n\geq 3\}$ *and where* $\beta_i=\frac{\alpha_i^2}{\sigma_i^2}$. *Then the determinant* $\det(\mathcal{I}(\mathbf{x}))$ *has an upper-bound of* $(\kappa^2 n^2\beta^2)/(4r^4)$ *and the determinant upper-bound can be achieved for this special case if and only if*

$$\sum_{i=1}^{n}\sin(2\phi_i(\mathbf{x}))=0\ \text{ and }\ \sum_{i=1}^{n}\cos(2\phi_i(\mathbf{x}))=0 \qquad (10)$$

which gives the optimal solution to the problems in Theorem 1.

Proof: If $\|\mathbf{x}-\mathbf{s}_i\|=\|\mathbf{x}-\mathbf{s}_j\|=r$ and $\beta_i=\beta_j=\beta$ is fixed (but arbitrary) for all $i,j\in\{1,\ldots,n\}$ then clearly $\frac{\beta^2}{r^4}$ can be factored out of the determinant (7) which leads to the upper-bound and the required condition. ■

Let us examine what the conditions given in Theorem 2 mean from a geometrical point of view. It is straightforward to verify that $\vartheta_{ij}=\vartheta_{ji}=\frac{2\pi}{n}$, $\forall i,j$ with $i-j=1$ is an optimal configuration when $\|\mathbf{x}-\mathbf{s}_i\|=\|\mathbf{x}-\mathbf{s}_j\|=r$ and $\beta_i=\beta_j=\beta$. This is not the only optimal sensor configuration. From Corollary 1 we know that reflecting any sensor about the emitter position does not effect the optimality. A notable optimal special case is $\vartheta_{ij}=\vartheta_{ji}=\frac{\pi}{n}$, $\forall i,j$ with $j-i=1$.

Corollary 2: If $\|\mathbf{x}-\mathbf{s}_i\|=\|\mathbf{x}-\mathbf{s}_j\|=r$ *and* $\beta_i=\beta_j=\beta$ *are fixed (but arbitrary)* $\forall i,j\in\{1,\ldots,n\geq 3\}$ *then the mean-squared-error is lower bounded with* $\mathrm{MSE}\geq(4r^2)/(n\kappa\beta)$ *and this lower bound is achieved if and only if (10) is satisfied.*

When $\|\mathbf{x}-\mathbf{s}_i\|\neq\|\mathbf{x}-\mathbf{s}_j\|$ and $\beta_i\neq\beta_j$ are arbitrarily fixed, the analysis is more involved; see [8], [9]. The next two theorems provide a general basis for finding the optimal localization geometries with $n\geq 3$ sensors and arbitrary range, path loss and noise variance values.

Theorem 3: Let ϕ_i, $\forall i\in\{1,\ldots,n>2\}$ *denote the angular positions of the sensors. Let* $r_i=\|\mathbf{x}-\mathbf{s}_i\|$ *be arbitrary but fixed for all* $i\in\{1,\ldots,n>2\}$. *The Fisher information determinant given in Theorem 1 is upper-bounded by*

$$\frac{\kappa^2}{4}\left(\sum_{i=1}^{n}\frac{\beta_i}{r_i^2}\right)^2 \qquad (11)$$

The upper-bound is achieved if and only if the conditions

$$\sum_{i=1}^{n}\frac{\beta_i\cos(2\phi_i)}{r_i^2}=0\ \text{ and }\ \sum_{i=1}^{N}\frac{\beta_i\sin(2\phi_i)}{r_i^2}=0 \qquad (12)$$

are satisfied by some ϕ_i, $\forall i\in\{1,\ldots,n>2\}$. *Furthermore, values of* ϕ_i, $\forall i\in\{1,2,\ldots,n>2\}$, *solving (12) can be found if and only if the following condition*

$$\frac{\beta_j}{r_j^2}\leq\sum_{i=1,i\neq j}^{n}\frac{\beta_i}{r_i^2} \qquad (13)$$

holds for all $j\in\{1,\ldots,n>2\}$.

Proof: Clearly, by equation (7), the upper bound is as stated and satisfaction of (12) is necessary and sufficient for the attainment of the upper bound. It remains to consider when there exist $\phi_i, \forall i \in \{1, 2, \ldots, n\}$, allowing satisfaction of (12). Equation (12) can be rewritten as

$$\sum_{i=1}^{N} \frac{\beta_i}{r_i^2} \begin{bmatrix} \cos(2\phi_i) \\ \sin(2\phi_i) \end{bmatrix} = \begin{bmatrix} 0 \\ 0 \end{bmatrix} \tag{14}$$

and suppose that the inequality condition (13) does not hold. Then clearly, (14) has no solution since one term on the left hand side will have a norm greater than the summed norms of all the other vectors. Hence, the necessity of (13) is established. The sufficiency of (13) is trivial to check. ■

The following corollary establishes the minimum MSE of an unbiased estimator given that the optimal geometry is characterized by the angular solutions to (12).

Corollary 3: If (13) holds and (12) is satisfied then the mean-square-error of an unbiased estimator obeys $\mathrm{MSE} \geq 4/(\kappa \sum_{i=1}^{n}(\beta_i/r_i^2))$.

A question remains as to how the optimal geometry is determined when (13) cannot be satisfied. The following result characterizes the optimal geometry for bearing-only localization when the key inequality condition (13) of Theorem 3 does not hold.

Theorem 4: Let $\phi_i, \forall i \in \{1, \ldots, n\}$ *denote the angular positions of the sensors. Let* $r_i = \|\mathbf{x} - \mathbf{s}_i\|$ *be arbitrary but fixed for all* $i \in \{1, \ldots, n > 2\}$. *If*

$$\frac{\beta_j}{r_j^2} > \sum_{i=1}^{n} \frac{\beta_i}{r_i^2}, \quad i \neq j \tag{15}$$

holds for some $j \in \{1, \ldots, n > 2\}$, *then the determinant given in Theorem 1 is upper-bounded by*

$$\kappa^2 \frac{\beta_j}{r_j^2} \sum_{i=1}^{n} \frac{\beta_i}{r_i^2}, \qquad i \neq j \tag{16}$$

and the upper-bound is achieved under (15) if and only if

$$\phi_j(\mathbf{p}) = \phi_i(\mathbf{p}) \pm \frac{\pi}{2} \tag{17}$$

for all $i \in \{1, \ldots, n\}/\{j\}$. *This implies* $\vartheta_{ji} = \vartheta_{ij} = \frac{\pi}{2}$, *for all* $i \in \{1, \ldots, n\}/\{j\}$ *and* $\vartheta_{ik} = \vartheta_{ki} = c\pi$, *where* $c \in \{0, 1\}$ *for all* $i, k \in \{1, \ldots, n\}/\{j\}$.

Proof: Firstly, the upper-bound will be derived via construction for range values satisfying (15). Refer back to equation (14) and note that under the assumption that (15) holds, the vector on the left hand side necessarily has a minimum norm equal to the difference

$$\frac{\beta_j}{r_j^2} - \sum_{i=1}^{n} \frac{\beta_i}{r_i^2}, \qquad i \neq j \tag{18}$$

Putting this value (18) into the determinant (7) leads to

$$\det(\mathcal{I}(\mathbf{x})) = \frac{\kappa^2}{4} \left[\left(\sum_{i=1}^{n} \frac{\beta_i}{r_i^2} \right)^2 - \left(\frac{\beta_j}{r_j^2} - \sum_{i=1,\ i \neq j}^{n} \frac{\beta_i}{r_i^2} \right)^2 \right] \tag{19}$$

for the same j and for all $i \in \{1, \ldots, n\}/\{j\}$. Rearranging the equation (19) leads to the upper-bound. Note that the upper-bound under the condition (15) has been explicitly constructed and it remains to show how this upper-bound can be achieved.

With no loss of generality, the condition (17) can be subsumed by the special case where $\phi_j = \frac{\pi}{2}$ for the same $j \in \{1, \ldots, n\}$ in (18) and $\phi_i = 0, \forall i \in \{1, \ldots, n\}/\{j\}$. This can be achieved by a global rotation of the coordinate system. Now note that $\sin(2\phi_j) = \sin(2\phi_i) = 0$ and $\cos(2\phi_j) = 1$ and $\cos(2\phi_i) = -1$ for those values of i and j specified previously. Putting these terms into the determinant (7) given in Theorem 1 part (ii) leads directly to (19) and thus proves the sufficiency of (17). The necessity of (17) follows easily when $n > 2$. ■

The following corollary establishes the minimum MSE of an unbiased estimator given that the optimal geometry is characterized by the anglular solutions to (17).

Corollary 4: If (15) holds and (17) is satisfied then the mean-square-error of an unbiased estimator obeys $\mathrm{MSE} \geq (\frac{r_j^2}{\kappa \beta_j} \sum_{i=1}^{n} \frac{\beta_i}{r_i^2})/(\sum_{i=1,\ i \neq j}^{n} \frac{\beta_i}{r_i^2})$.

If (15) is satisfied for some sensor j, then that sensor j is much closer to the target relative to all the other sensors. Moreover, that same sensor j should be placed at a right angle to all other sensors, i.e the other sensors should be collinear. Alternatively, when (13) in Theorem 3 holds, then the condition (12) leads to the optimal sensor configuration. However, finding values of $\phi_i, \forall i \in \{1, 2, \ldots, n\}$, that solve (12) is not straightforward, in general, for an arbitrary number of sensors n and for fixed but arbitrary ranges $r_i\ \forall i \in \{1, 2, \ldots, n\}$.

The next result provides a powerful tool with which to build optimal sensor configurations using flexible positioning rules.

Corollary 5: Consider $n \geq 4$ *sensors tasked at localizing a single target and assume that* $r_i = \|\mathbf{x} - \mathbf{s}_i\|$ *is arbitrary but fixed,* $\forall i \in \{1, \ldots, n \geq 4\}$. *Denote the set of* $n \geq 4$ *sensors by* $\mathcal{V}$ *and assume further that (13) is satisfied for the entire set of sensors* $i \in \mathcal{V}$. *Now assume that* $\mathcal{V}$ *can be split into some arbitrary number* m *of subsets* $\mathcal{B}_i$ *such that* $\mathcal{B}_i \cap \mathcal{B}_j = \emptyset$ *and* $|\mathcal{B}_i| \geq 2$, $\forall i, j \in \{1, \ldots, m\}$ *with* $i \neq j$. *Moreover, assume the condition (13) is satisfied by the subset group of range values for the sensors in* $\mathcal{B}_i$. *Then, an optimal* m *sensor configuration can be obtained by placing all subsets of sensors* $\mathcal{B}_i, \forall i \in \{1, \ldots, m\}$ *in optimal angular positions as specified by (12) in Theorem 3.*

If Corollary 5 can be employed, then an infinite number of sensor configurations can be obtained by rotating any sensor subset $\mathcal{B}_i$ relative to (and independent of) any other sensor subset $\mathcal{B}_j$ with $i \neq j$. Hence, for $n \geq 4$ bearing-only sensors there *can* exist an infinite number of optimal sensor configurations. Note that Corollary 5 is thus a powerful tool when it comes to the problem of optimal sensor placement. Again, we highlight that an equi-angular spacing is almost never optimal and is in fact never necessary for optimality. Moreover, an optimal configuration can always be found with all sensors positioned on a common half-plane.

We also note the striking similarity between the optimal geometry for RSS-based and bearing-only localization; e.g. see [8]. We will now completely and rigorously examine the practically important case involving $n = 3$ sensors.

V. Complete Study with Three Sensors

The RSS-based localization problem with three sensors is not arbitrary since a minimum of three sensors is required to uniquely localize the emitter. It is practically reasonable to assume only three sensors will cooperate in localizing individual emitters in modern wireless networks [2], [3], [6].

The following contribution completely characterizes the geometry for RSS-based localization with three sensors.

Theorem 5: Let $\gamma_i = \beta_i/\|\mathbf{x}-\mathbf{s}_i\|^2$ *and* $\gamma_{ij} = \gamma_i\gamma_j > 0$ *be arbitrary but fixed* $\forall i \in \{1,2,3\}$. *The optimal sensor configuration is not unique. Every optimal angular separation* ϑ_{12}, ϑ_{13} *and* ϑ_{23} *can be obtained by first solving*

$$\begin{aligned}\vartheta_{12} &= \frac{1}{2}\arccos\left(\frac{\gamma_{13}^2\gamma_{23}^2-\gamma_{12}^2\gamma_{23}^2-\gamma_{12}^2\gamma_{13}^2}{2\gamma_{12}^2\gamma_{13}\gamma_{23}}\right)\\ \vartheta_{13} &= \frac{1}{2}\arccos\left(\frac{\gamma_{12}^2\gamma_{23}^2-\gamma_{12}^2\gamma_{13}^2-\gamma_{13}^2\gamma_{23}^2}{2\gamma_{12}\gamma_{13}^2\gamma_{23}}\right)\\ \vartheta_{23} &= \pi-\vartheta_{12}-\vartheta_{13}\end{aligned}$$

when the $\arccos(\cdot)$ *are real (which occurs simultaneously for* ϑ_{12} *and* ϑ_{13}*) and then by an application of Corollary 1 (giving the first optimal solution set). If no real solution for both* ϑ_{12} *and* ϑ_{13} *exists then* $\det(\mathcal{I}(\mathbf{x}))$ *is maximized when*

$$\begin{cases}\vartheta_{ij}=\frac{\pi}{2}, & \text{if } \gamma_{ij}>\gamma_{kl},\quad \forall kl\in\{12,13,23\}/\{ij\}\\ \vartheta_{ij}=0 \text{ or } \pi, & \text{otherwise}\end{cases}$$

where now (in the second solution set) we have automatically accounted for sensor reflections as per Corollary 1.

Proof: From Theorem 1 part (iv) we can derive the following optimization problem

$$\underset{A,B}{\operatorname{argmax}}\ \gamma_{12}\sin^2(A)+\gamma_{13}\sin^2(B)+\gamma_{23}\sin^2(B-A) \quad (20)$$

where $A=(\phi_2-\phi_1)$, $B=(\phi_3-\phi_1)$ and $\gamma_{ij}=\gamma_i\gamma_j>0$ are arbitrary constants with $\gamma_i=\beta_i/\|\mathbf{x}-\mathbf{s}_i\|^2$. Taking the gradient with respect to A and B and rearranging leads to

$$\begin{aligned}\gamma_{12}\sin(2A)+\gamma_{13}\sin(2B) &= 0 \quad (21)\\ \sin(2A)\left[\frac{\gamma_{12}}{\gamma_{23}}+\frac{\gamma_{12}}{\gamma_{13}}\cos(2A)+\cos(2B)\right] &= 0 \quad (22)\\ \sin(2B)\left[\frac{\gamma_{13}}{\gamma_{23}}+\frac{\gamma_{13}}{\gamma_{12}}\cos(2B)+\cos(2A)\right] &= 0 \quad (23)\end{aligned}$$

From (21) we note that if $\sin(2A)=0$ then $\sin(2B)=0$ or if $\sin(2A)\neq 0$ then $\sin(2B)\neq 0$. Thus, $\sin(2A)=0$ and $\sin(2B)=0$ implies $A=\frac{c_A\pi}{2}$ and $B=\frac{c_B\pi}{2}$ with $c_A,c_B\in\mathbb{N}$. Also, if $\sin(2A)\neq 0\neq\sin(2B)$ then (22) and (23) lead to

$$\begin{aligned}A &= \frac{1}{2}\arccos\left(\frac{\gamma_{13}^2\gamma_{23}^2-\gamma_{12}^2\gamma_{23}^2-\gamma_{12}^2\gamma_{13}^2}{2\gamma_{12}^2\gamma_{13}\gamma_{23}}\right) \quad (24)\\ B &= \frac{1}{2}\arccos\left(\frac{\gamma_{12}^2\gamma_{23}^2-\gamma_{12}^2\gamma_{13}^2-\gamma_{13}^2\gamma_{23}^2}{2\gamma_{12}\gamma_{13}^2\gamma_{23}}\right) \quad (25)\end{aligned}$$

where the $\arccos(\cdot)$ are simultaneously real. We now have two mutually exclusive sets of critical points corresponding to $\sin(2A)=\sin(2B)=0$ and $\sin(2A)\neq 0\neq\sin(2B)$ respectively. If $A=\frac{c_A\pi}{2}$ and $B=\frac{c_B\pi}{2}$ then $\cos(2A)=\pm 1$ and $\cos(2B)=\pm 1$ which lie on the boundary of where (24) and (25) are real. The maximizing values for A and B in (20) must change continuously for continuous changes in γ_{ij}. Thus, if $A=\frac{c_A\pi}{2}$ and $B=\frac{c_B\pi}{2}$ solve (20) then they do so for all γ_{ij} or they do so only when no real solutions exist via (24) and (25). Now it can be verified that if $\gamma_{12}=\gamma_{13}=\gamma_{23}$ then both (24) and (25) give real solutions for A and B which lead to a greater value of (20) when compared to $A=\frac{c_A\pi}{2}$ and $B=\frac{c_B\pi}{2}$. Hence, it follows that (24) and (25) maximize (20) when the solutions are real. Otherwise, the maximizing solutions of (20) are $A=\frac{c_A\pi}{2}$ and $B=\frac{c_B\pi}{2}$ with $c_A,c_B\in\mathbb{N}$. It is easy to find the relationship between the ϑ_{ij} and A and B when (24) and (25) give real solutions. When $A=\frac{c_A\pi}{2}$ and $B=\frac{c_B\pi}{2}$ maximize (20), then one of the $\sin^2(\cdot)$ terms in (20) must be zero while the other two $\sin^2(\cdot)$ terms are one. In this case if $\gamma_{ij}<\gamma_{kl}$ for some $i,j\in\{1,2,3\}$ and $\forall k,l\in\{1,2,3\}$ with $ij\neq kl$ then the $\gamma_{ij}\sin^2(\cdot)$ term in (20) should be zero in order to solve the problem (20) and the ϑ_{ij} follow. ■

We have completely characterized the sensor-emitter geometry with $n=3$ sensors for RSS-based localization. Note the solutions given when the $\arccos(\cdot)$ terms in Theorem 5 are real correspond to the solutions of (12) given in Theorem 3. Now, the second solution set in Theorem 5 are valid if and only if (15) in Theorem 4 holds. That is, the two solution sets in Theorem 5 are the exactly derived solutions to the two general condition sets outlined in Theorems 3 and 4 in the general n sensor case.

Corollary 6: Assume $\gamma_i=\beta_i/\|\mathbf{x}-\mathbf{s}_i\|^2$ *is fixed such that the* $\arccos(\cdot)$ *terms in Theorem 5 are real. The mean-squared-error is lower bounded with* $\mathrm{MSE}\geq 4/(\kappa(\gamma_1+\gamma_2+\gamma_3))$ *and this lower bound is achieved if and only if the angles* ϑ_{ij} *are given by the first solution set in Theorem 5.*

Corollary 7: Assume $\gamma_i=\beta_i/\|\mathbf{x}-\mathbf{s}_i\|^2$ *are fixed such that no real solution of the* $\arccos(\cdot)$ *terms in Theorem 5 exist. Then* $\gamma_i>\gamma_j+\gamma_k$ *for some* $i\neq j,k$. *The mean-squared-error is lower bounded with* $\mathrm{MSE}\geq(\gamma_i+\gamma_j+\gamma_k)/(\kappa\gamma_i(\gamma_j+\gamma_k))$ *and this lower bound is achieved if and only if the angles* ϑ_{ij} *are given by the second solution set in Theorem 5.*

Now let $\beta_i=1$ and $\gamma_i=1/\|\mathbf{x}-\mathbf{s}_i\|$. Then the conditions in Theorem 5 are in terms of the relative sensor-emitter ranges $r_i=\|\mathbf{x}-\mathbf{s}_i\|$. Consider now the illustration in Fig. 2.

Fig. 2 shows the variation of the optimal geometry as r_1 changes from one extreme $r_1<<r_2=r_3$ to the other $r_1>>r_2=r_3$ with $\beta_i=\beta_j=1$. The particular ranges and ϑ_{ij} (in degrees) are given in the figure titles. In Fig. 2(a), the ranges are such that both $\arccos(\cdot)$ functions in Theorem 5 are not real and thus the optimal geometry (shown) is such that sensor 1 forms right angles with sensors 2 and 3. At the other extreme in Fig. 2(d), the ranges are such that $r_1>>r_2=r_3$ and thus sensor 2 and 3 are (almost) at right angles with sensor 1 splitting the difference between them. Indeed, from Theorem 5 we see that as $r_1\to\infty$ then $\vartheta_{23}\to\frac{\pi}{2}$. Sensor reflections over the emitter do not change the optimality of the geometry. Importantly, if the sensor-target ranges are not equivalent, then placing the sensors with an equi-angular spacing around the target is never optimal. Actually, this form of spacing is never necessary for optimality in any case.

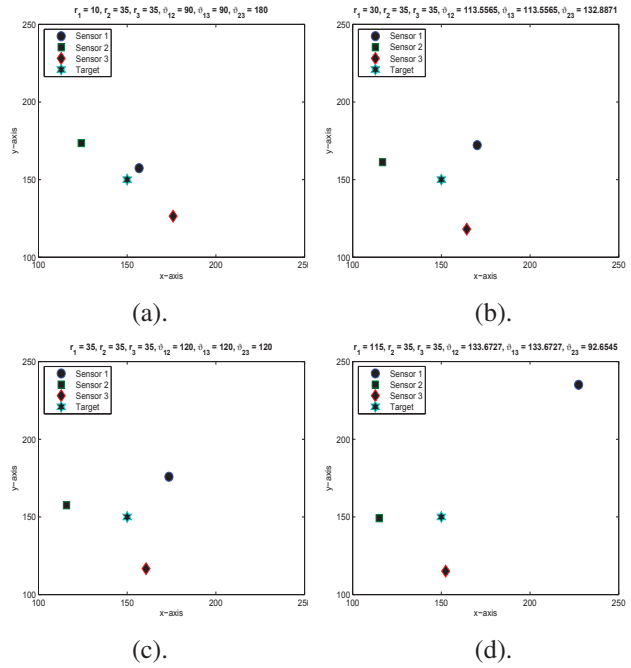

Fig. 2. This figure illustrates the different optimal sensor-target geometries for different ranges r_i from sensor i to the emitter. We have assumed $\beta_i = \beta_j = 1$, $\forall i, j \in \{1, 2, 3\}$. In this illustration, only r_1 changes and the ranges and ϑ_{ij} (in degrees) are given in the figure titles. In part (a) the range $r_1 << r_2 = r_3$ means that both $\arccos(\cdot)$ functions in Theorem 5 are not real and hence the optimal sensor geometry (shown) is when $\vartheta_{12} = \vartheta_{13} = \frac{\pi}{2}$ and $\vartheta_{23} = \pi$ (or $\vartheta_{23} = 0$ is equivalently valid but not shown). In part (b) the ranges are $r_1 < r_2 = r_3$ and both $\arccos(\cdot)$ functions in Theorem 5 are real and hence the optimal geometry (shown) is not a right angle geometry but rather ϑ_{12} and ϑ_{13} are given by the $\arccos(\cdot)$ functions and ϑ_{23} follows immediately. In part (c) we see that when $r_1 = r_2 = r_3$ the optimal sensor geometry (shown) is equally spaced around the emitter. In part (d) we want to illustrate that as $r_1 >> r_2 = r_3$ the angle ϑ_{23} approaches $\frac{\pi}{2}$ as r_1 approaches ∞. Indeed, when $r_1 >> r_2 = r_3$, part (d) illustrates that we can easily approximate the optimal geometry as such. Recall from Corollary 1 that sensor reflections over the emitter do not change the optimality of the geometry and hence this figure illustrates only the most intuitive examples.

VI. Discussion

We have provided a rigorous theoretical analysis of the sensor-target geometry which indicates that commonly held assumptions are not generally valid. There are obvious *practical* advantages in developing a deep theoretical understanding of the sensor-target geometry and its affect on localization performance. The results in this paper can be used to better place sensors given approximate knowledge of the targets region of location. Indeed, knowledge of the targets region of location is often available as a function of the commonly known sensor range and field-of-view.

Interestingly, the MSE (or RMSE) lower bound decreases with an increase in the path loss exponent (given a fixed geometry of course) [3].

VII. Conclusion

In this paper we explored the optimality of the relative sensor-emitter geometry for signal strength based localization. We completely characterized the geometry for $n = 2$ and importantly for $n = 3$ sensors. Moreover, we provided a number of explicit, and powerful, results that can be used to optimally arrange an arbitrary number n of sensors given arbitrary system parameters. No existing work in the literature has analyzed the optimal geometry for RSS-based localization.

VIII. Acknowledgment

The authors are supported by the Swedish Foundation for Strategic Research (SSF) through the Center for Autonomous Systems (CAS) and also via the EU FP7 project 'CogX'.

References

[1] V. Erceg, L. Greenstein, S. Tjandra, S. Parkoff, A. Gupta, B. Kulic, A. Julius, and R. Jastrzab. An empirically based path loss model for wireless channels in suburban environments. *IEEE Journal on Selected Areas in Communications*, 17(7):1205–1211, July 1999.

[2] J. Aspnes, T. Eren, D.K. Goldenberg, A.S. Morse, W. Whiteley, Y.R. Yang, B.D.O. Anderson, and P.N. Belhumeur. A theory of network localization. *IEEE Transactions on Mobile Computing*, 5(12):1663–1678, December 2006.

[3] N. Patwari, J.N. Ash, S. Kyperountas, A.O. Hero III, R.L. Moses, and N.S. Correal. Locating the nodes: Cooperative localization in wireless sensor networks. *IEEE Signal Processing Magazine*, 22(4):54–69, July 2005.

[4] N. Patwari, A.O. Hero, M. Perkins, N.S. Correal, and R.J. O'Dea. Relative location estimation in wireless sensor networks. *IEEE Transactions on Signal Processing*, 51(8):2137–2148, August 2003.

[5] M. McGuire, K.N. Plataniotis, and A.N. Venetsanopoulos. Data fusion of power and time measurements for mobile terminal location. *IEEE Transactions on Mobile Computing*, 4(2):142–153, March-April 2005.

[6] Z.R. Zaidi and B.L. Mark. Real-time mobility tracking algorithms for cellular networks based on kalman filtering. *IEEE Transactions on Mobile Computing*, 4(2):195–208, March-April 2005.

[7] S. Martinez and F. Bullo. Optimal sensor placement and motion coordination for target tracking. *Automatica*, 42(4):661–668, 2006.

[8] A.N. Bishop, B. Fidan, B.D.O. Anderson, K. Dogancay, and P.N. Pathirana. Optimality analysis of sensor-target geometries in passive localization: Part 1 - Bearing-only localization. In *Proceedings of the 3rd International Conference on Intelligent Sensors, Sensor Networks and Information Processing (ISSNIP)*, December 2007.

[9] A.N. Bishop, B. Fidan, B.D.O. Anderson, P.N. Pathirana, and K. Dogancay. Optimality analysis of sensor-target geometries in passive localization: Part 2 - Time-of-arrival based localization. In *Proceedings of the 3rd ISSNIP Conference*, December 2007.

[10] A.N. Bishop, B. Fidan, K. Dogancay, B.D.O. Anderson, and P.N. Pathirana. Exploiting geometry for improved hybrid AOA/TDOA based localization. *Signal Processing*, 88(7):1775–1791, July 2008.

[11] A.N. Bishop, B. Fidan, B.D.O. Anderson, K. Dogancay, and P.N. Pathirana. Optimal range-difference-based localization considering geometrical constraints. *IEEE Journal of Oceanic Engineering*, 33(3):289–301, July 2008.

[12] H.L. Van Trees. *Detection, Estimation and Modulation Theory*. John Wiley and Sons, Inc., New York, NY, 1968.

[13] A.N. Bishop and P.N. Pathirana. Optimal trajectories for homing navigation with bearing measurements. In *Proceedings of the 2008 International Federation of Automatic Control Congress*, July 2008.

[14] A.J. Weiss. On the accuracy of a cellular location system based on RSS measurements. *IEEE Transactions on Vehicular Technology*, 52(6):1508–1518, November 2003.

[15] A. Dogandzic and P.P. Amran. Signal-strength based localization in wireless fading channels. In *Proceedings of the 38th Asilomar Conference on Signals, Systems and Computers*, November 2004.

[16] F. Bouchereau and D. Brady. Bounds on range-resolution degradation using RSSI measurements. In *IEEE International Conference on Communications (ICC 2004)*, June 2004.

[17] A. Catovic and Z. Sahinoglu. The Cramer-Rao bounds of hybrid TOA/RSS and TDOA/RSS location estimation schemes. *IEEE Communication Letters*, 8(10):626–628, October 2004.

[18] R.A. Horn and C.R. Johnson. *Matrix Analysis*. Cambridge University Press, New York, NY, 1985.